Available online at www.sciencedirect.com
SCIENCE DIRECT®
Chemical Physics 297 (2004) 323–332
Chemical Physics
www.elsevier.com/locate/chemphys

Intramolecular hydrogen bond in molecular and proton-transfer forms of *Schiff* bases

A. Filarowski [a,*], A. Koll [a], A. Karpfen [b], P. Wolschann [b]

[a] *Institute of Chemistry, University of Wrocław, 14 F, Joliot-Curie Str., Wrocław PL-50383, Poland*
[b] *Institute of Theoretical Chemistry and Structural Biology, Universität Wien, Währinger Straße 17, Vienna A-1090, Austria*

Received 5 March 2003; accepted 22 October 2003

Abstract

The force field and structural parameters modifications upon the formation of intramolecular hydrogen bond and proton transfer reaction in *N*-methyl-2-hydroxybenzylidene amine (HBZA) are determined on the basis of ab initio and DFT calculations. Reliability of the calculations is verified by comparing of the theoretical vibrational spectra with those experimentally determined in the gas phase. A model of resonance interactions is applied and the quantitative contribution of *ortho*-quinoid structure in the particular conformers is estimated. A comparison is also made to the systems without π-electron coupling (*Mannich* bases).

Keywords: Ab initio and DFT calculations; *Schiff* bases intramolecular hydrogen bond; Keto forms; Gas phase IR spectra

1. Introduction

The *ortho*-hydroxy *Schiff* bases belong to the group of compounds forming the intramolecular hydrogen bonds arising ever growing interest due to π-electron coupling between the acid and base centres [1–10]. Such systems are interesting both from the theoretical and experimental point of view [1,2]. The intramolecular proton transfer reaction proceeds comparatively easily in these compounds. Therefore, one can observe the double fluorescence [11–13], thermochromic and photochromic properties [14]. These compounds are potential materials for molecular memory and optical switch device [15] or fluorescent probes of biological systems [16]. They are used as models of biological systems [17,18]. Intramolecular π-electron coupling leads to the strengthening of the hydrogen bonds in these systems (resonance assisted hydrogen bond – RAHB) [19]. A comparison of IR investigations of *Schiff* bases and structurally similar *Mannich* bases were performed [20]. It was shown that the *ν*(OH) stretching bands reveal a larger frequency shift in *Schiff* bases. However, the integrated intensities of the same bands appeared to be smaller for *Schiff* bases than for *Mannich* bases with the same acid base properties of interacting centres. It demonstrates that nature of hydrogen bonding interactions in *Schiff* bases is to some extent different than in intramolecular hydrogen bonds without π-electron coupling.

Explanation of an origin of these differences is a main task of this paper. In the *Mannich* bases study we have found [21,22] that the most effective way to analyse the consequences of the formation of the intramolecular hydrogen bonding is to monitor the structural differences between closed and open conformers. In case of *Schiff* bases calculations of related forms of proton transfer (PT) tautomer are possible because PT stationary states are formed. It was stated [21,22] that the formation of intramolecular hydrogen bond leads to structural and dynamic (force constants) changes of *ortho*-quinoid pattern, despite the fact that electronic coupling in *Mannich* bases is seriously reduced by the $-CH_2-$ bridge between the acid and base centres. Therefore, it was interesting to make comparison with *Schiff* bases revealing direct coupling between these centres. Proton transfer equilibria and structural effects

* Corresponding author. Fax: +48-71-328-2348.
E-mail address: afil@wchuwr.chem.uni.wroc.pl (A. Filarowski).

0301-0104/$ - see front matter © 2003 Elsevier B.V. All rights reserved.
doi:10.1016/j.chemphys.2003.10.035

of the formation of intramolecular hydrogen bond with π-electron coupling were discussed in literature already [23–31]. The systems with large π-electron delocalization, like *Schiff* bases, can be described with the help of resonance theory [32]. We aim at estimation of the content of keto resonance forms to characterise the species participating in equilibrium.

2. Experimental and computational

Synthesis of *Schiff* base from the stoichiometric mixture of salicylaldehyde and methylamine in methanol was performed according to [33].

IR gas phase spectra of HBZA were obtained at room temperature in 10 cm length cell with CsJ windows on the Avatar 360 Nicolet FT-IR spectrometer. Spectral resolution was 2 cm^{-1}. The spectra were also measured for the OD deuterated samples. Raman spectra were recorded on a Nicolet FT Raman module coupled to Nicolet Magna 860 FT-IR spectrometer.

The quantum chemical calculations were carried out with the GAUSSIAN 94 program package [34]. The geometry optimization was performed at MP2 [35] and B3LYP [36] levels with 6-31G(d,p) basis set [37]. The IR frequencies and intensities were calculated by B3LYP/6-31G(d,p) and B3LYP/6-311++G(d,p) methods, and internal coordinates were defined, which allowed assignment of transitions and effects of deuteration. Calculated by Gaussian program spectra were related to the experimental ones by homemade program with assumed Lorentz band shape and 8 cm^{-1} half width. In such an approach we intend to verify the utility of B3LYP/6-31(d,p) method in description of the intramolecular hydrogen bond with π-electron coupling. In the structural questions MP2 method was applied, which directly treats the electron correlation effects, and in spectroscopic question by extension the basis set and including diffuse functions, while the MP2 approach has known deficits in IR bands assignments (see further).

3. Results and discussion

To monitor the consequences of the formation of intramolecular hydrogen bonding the structural differences between the closed and open conformers are discussed. The effect of mutual non-hydrogen bonded interaction between substituents is eliminated to a high extent in such an approach. The open forms were obtained by the rotation of the methylimine group on 180° around the C_{aryl}–C_{alkyl} bond (see Scheme 1) as well as the simultaneous rotation of the O–H bond around the C–O axis on 180° in molecular form and subsequent optimization.

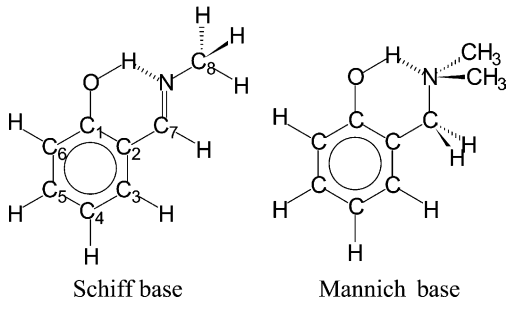

Scheme 1.

3.1. Comparing of the experimental and calculated IR spectra

With the aim of the study of structural and spectroscopic consequences of the formation of hydrogen bond and proton transfer by theoretical methods the first step undertaken in our study was verification of these methods in reproduction of experimentally obtained IR gas phase, Raman and deuterated spectra of *N*-methyl-2-hydroxybenzylidene amine.

The experimental data are given in Table 1 together with the results of B3LYP/6-31G(d,p) and B3LYP/6-311++G(d,p) calculations, cf. [23,38]. The second basis set was used to explain the role of diffuse functions in description of the spectra of benzylidene derivatives with large electron delocalization.

Theoretical bands' assignment was done by potential energy distribution methods (PED) [39]. Attributing of the calculated spectra to the experimental ones was completed by comparing of the frequencies, intensity pattern, Raman intensities and the consequences of OH group deuteration as well by comparing with literature data [40,41]. Non-standard [42] frequency scaling factors were calculated by dividing of the particular experimental and calculated frequencies of phenol [23] within the finger print range. The *ν*(C–H) and *ν*(OH) bands will not be discussed subsequently because of its different (larger) unharmonicity [23]. After frequency scaling, both calculation methods give spectra similar to each of other and to the experimental ones (see Fig. 1 and footnotes of Table 1). The content of normal modes is expressed according to symmetry coordinates defined in Table 2. Bands assignment can be supported by a good coincidence with classical valence force field results [43] for benzylidene compounds [40,41]. Some differences result obviously from 2-OH group substitution in HBZA compound.

Conclusions of this part are as follows. Both B3LYP/6-31G(d,p) and B3LYP/6-311++G(d,p) methods give a very good reproduction of the experimental spectra. Introducing of the diffuse functions does not significantly influence the bands' positions, or the content of normal modes. One can say that DFT B3LYP/6-31G(d,p) method was positively verified in description

Table 1
Experimental (IR-gas phase, R-oil) and calculated at B3LYP/6-31G(d,p) and B3LYP/6-311++G(d,p) levels, vibrational frequencies ν (cm^{-1}) and intensities A (km mol^{-1}) with assignment (PED, %) for HBZA molecular form

Experimental	Calculated		B3LYP/6-31G(d,p)	Calculated		B3LYP/6-311++G(d,p)
IR ν (A) R ν (A)	ν[a] 0.9772	ν (A)	PED (%)	ν[a] 0.9913	ν (A)	PED (%)
466 (25)	466	477 (2)	δ(CO) (61), δ_{im}(CC) (14), δ(CNC) (10)	472	476 (2)	δ(CO) (59), δ(CNC) (14), δ_{im}(CC) (11)
468 (30)						
556 (20)	558	571 (3)	α(CCC) (65), δ_{im}(CC) (11), r(CC)(7)	565	570 (3)	α(CCC) (64), δ_{im}(CC) (11), r(CC) (8), ν(CO) (5)
561 (45)						
646 (25)	646	661 (9)	α(CCC) (55), δ(CCN) (16)	655	661 (10)	α(CCC) (55), δ(CCN) (16)
647 (25)						
753 (105)[c]	751	769 (57)	γ(CH) (88), γ(CO) (8)	755	762 (85)	γ(CH) (89), γ(CO) (7)
782, sh	782	800 (8)	r(CC) (48), ν(CO) (11), δ(CCN) (6), δ(CNC) (6),	787	794 (9)	r(CC) (46), ν(CO) (12), α(CCC) (8), δ(CCN) (6),
782 (55)			α(CCC) (5), ν_{im}(CC) (5)			δ(CNC) (6), ν_{im}(CC) (5)
797 (60)	839	859 (73)	γ(COH) (57), γ(CH) (12), γ(CO) (7), τ(CCC) (6)[b]	844	851 (60)	γ(COH) (48), γ(CH) (29), γ(CO) (7), τ(CCC) (5)
895 (35)[c]	885	905 (10)	α(CCC) (64), δ(CCN) (11), ν_{im}(CC) (6), ν(CO) (6)	897	905 (13)	α(CCC) (59), δ(CCN) (11), ν_{im}(CC) (7), ν(CO) (7)
966 (30)[c]	973	996 (7)	γ_{im}(CH) (60), ν(CN) (10), ν_{im}(CC) (7), γ(CH) (6),	981	990 (11)	γ_{im}(CH) (58), ν(CN) (10), γ(CH) (7), ν_{im}(CC) (6),
			γ_{im}(CC) (5)			γ_{im}(CC) (6)
1008 (60)[c]	1011	1035 (24)	ν(NC) (53), δ(CCN) (9), δ(NCH_3) (7), r(CC) (7)	1016	1025 (25)	ν(NC) (55), δ(CCN) (9), δ(NCH_3) (7), r(CC) (6)
1036 (30)	1039	1063 (7)	r(CC) (52), β(CH) (18), ν(NC) (13)	1047	1056 (9)	r(CC) (55), β(CH) (19), ν(NC) (11)
1037 (110)						
1147 (40)	1156	1183 (18)	β(CH) (77), r(CC) (8)	1168	1178 (18)	β(CH) (78), r(CC) (8)
1151 (40)						
1210 (45)	1214	1242 (38)	ν_{im}(CC) (25), r(CC) (22), β(CH) (17), δ_{im}(CH) (10)	1221	1232 (36)	r(CC) (27), ν_{im}(CC) (24), β(CH) (18), δ_{im}(CH) (10)
1212 (40)						
1242 (90)	1245	1274 (8)	β(CH) (42), r(CC) (16), δ_{im}(CC) (6), δ(CO) (6),	1253	1264 (4)	β(CH) (42), r(CC) (17), ν_{im}(CC) (6), ν(CO) (6), δ(CO)
			δ_{im}(CH) (5), δ_{im}(CC) (5)			(5)
1283 (100)[c]	1307	1338 (66)	ν(CO) (40), α(CCC) (12), β(CH) (11), r(CC) (8)	1303	1314 (94)	ν(CO) (41), α(CCC) (14), β(CH) (10)
1318 (20)	1341	1372 (3)	r(CC) (75), β(CH) (6)	1340	1352 (2)	r(CC) (75), β(CH) (6)
1316 (80)						
1373 (40)[c]	1375	1407 (15)	δ_{im}(CH) (58), ν_{im}(CC) (8), ν(CN) (6)	1383	1395 (16)	δ_{im}(CH) (58), ν_{im}(CC) (8), ν(CN) (6), β(CH) (5)
1405 (80)	1420	1453 (31)	δ(NCH_3) (85), ν(NC) (5)	1427	1440 (17)	δ(NCH_3) (88), ν(NC) (5)
				1464	1477 (7)	δ(NCH_3) (97)
1412 (80)	1438	1472 (52)	β(CH) (29), δ(COH) (27), r(CC) (23), ν_{im}(CC) (6)	1442	1455 (49)	δ(COH) (30), β(CH) (28), r(CC) (20), ν_{im}(CC) (6)[d]
1457 (80)	1473	1507 (41)	δ(NCH_3) (50), r(CC) (11), ν(CO) (6)	1479	1492 (61)	r(CC) (26), δ(NCH_3) (24), β(CH) (13), ν(CO) (8)
1453 (50)						
1465 (45)	1484	1519 (25)	δ(NCH_3) (27), β(CH) (20), r(CC) (19), ν(CO) (11)	1490	1503 (9)	δ(NCH_3) (53), β(CH) (10), r(CC) (6)
1494 (100)[c]	1517	1552 (60)	r(CC) (26), β(CH) (25), δ(COH) (25)	1521	1534 (52)	β(CH) (26), δ(COH) (24), r(CC) (24)[d]
1589 (67)	1601	1638 (68)	r(CC) (49), δ(COH) (18), β(CH) (9), α(CCC) (5)	1604	1618 (57)	r(CC) (52), δ(COH) (15), β(CH) (10), α(CCC) (7)[d]
1583 (55)						
	1643	1681 (82)	r(CC) (52), δ(COH) (12), α(CCC) (8), β(CH) (6)	1648	1662 (93)	r(CC) (52), δ(COH) (11), α(CCC) (9), β(CH) (6)
1648 (200)	1677	1716 (201)	r(CN) (63), δ_{im}(CH) (11), ν_{im}(CC) (6), δ_{im}(CC) (5)	1680	1695 (200)	r(CN) (64), δ_{im}(CH) (11), ν_{im}(CC) (6)
1639 (200)						
2741 (46)	2931	2999 (99)	ν(CH) (99)	2958	2984 (85)	ν(CH) (98)
2790 (61)	2950	3019 (86)	ν_{im}(CH) (97)	2974	3000 (87)	ν_{im}(CH) (96)
2867 (49)	3011	3081 (29)	ν(CH) (99)	3037	3064 (26)	ν(CH) (99)
2903 (47)	3023	3094 (21)	ν(CH) (100)	3049	3076 (16)	ν(CH) (100)
3013 (20)	3098	3170 (18)	ν_{ar}(CH) (98)	3129	3156 (4)	ν_{ar}(CH) (96)
3053 (10)	3112	3185 (5)	ν_{ar}(CH) (96)	3141	3169 (16)	ν_{ar}(CH) (99)

Table 1 (*continued*)

Experimental		Calculated		B3LYP/6-31G(d,p)	Calculated		B3LYP/6-311++G(d,p)
IR ν (*A*)	R ν (*A*)	ν^a 0.9772	ν (*A*)	PED (%)	ν^a 0.9913	ν (*A*)	PED (%)
3076 (22)		3135	3208 (19)	ν_{ar}(CH) (93)	3162	3190 (23)	ν_{ar}(CH) (93)
3179 (6)		3142	3215 (12)	ν_{ar}(CH) (99)	3167	3195 (329)	ν(OH) (84), ν_{ar}(CH) (11)
2990[a]		3070	3142 (396)	ν(OH) (98)	3169	3197 (100)	ν_{ar}(CH) (86), ν(OH) (12)

Only internal coordinates contributing by more than 5% to the normal coordinates are reported.
[a] Very broad absorption band; values in the second and fifth column are multiplied by frequency correction factors [42].
[b] Experimental band disappears upon deuteration.
[c] No Raman band, which is in agreement with calculations.
[d] Low frequency shift upon deuteration both in experiment and calculations.

Fig. 1. Experimental (**1** – HBZA, **4** – HBZA(OD)) and calculated (**2** – B3LYP/6-31G(d,p) HBZA, **3** – B3LYP/6-311++G(d,p) HBZA; **5** –B3-LYP/6-31G(d,p) HBZA(OD), **6** – B3LYP/6-311++G(d,p) HBZA (OD)) infrared spectra of HBZA.

of the properties of intramolecular hydrogen bond in molecules with π-electron coupling.

3.2. The phenol ring distortion

It was found that formation of the intramolecular hydrogen bond in *Mannich* bases (AP, DMAP) [21,22] encourages bond differentiation in the pattern characteristic for *ortho*-quinoid resonance structure, suggesting electron coupling between substituents. The results of HBZA structure calculations are given in Table 3. The atoms' labelling is in accordance with Scheme 1. The structural parameters can be directly compared to related values for DMAP [22]. In this paper the same methods of calculations were used as for *Mannich* bases [21,22].

The results presented in Table 3 show, that ring bonds alternation increases very strongly after the proton transfer, which is in accordance with the expected increase of the contribution of *ortho*-quinoid resonance form. Such conformers are often described in literature as "keto" forms.

Table 2
Definitions of internal coordinates used in the potential energy distribution (PED) analysis for the assignment of the vibrational spectra of the HBZA

r(CC) – ring stretching
ν_{ar}(CH) – stretching of the C–H bond centered on a carbon atom in the ring
ν(CH) – stretching of aliphatic C–H bond
ν(OH) – stretching of the O–H bond
ν(CO) – stretching of the C–O bond
ν(CN) – stretching of the C7=N bond
ν(NC) – stretching of the N–C8 bond
ν_{im}(CC) – stretching of the C2–C7 bond
ν_{im}(CH) – stretching of the C7–H bond
α(CCC) – in plane bending of the C–C–C chain in the aromatic ring
β(CH) – in plane bending (the change in angle between the C–H bond and the line, bisecting the angle defined by three carbon atoms in the ring)
δ_{im}(CC) – in plane bending of the C2–C7 bond
δ_{im}(CH) – in plane bending of the C7–H bond
δ(CNC) – in plane bending of the C7=N–C8 chain
δ(CO) – in plane bending of the C–O bond
δ(COH) – in plane bending of the C–O–H chain
δ(CCN) – in plane bending of the C2–C7=N chain
γ(CH) – out of plane bending of the C–H bond (the change in angle between the C–H bond and plane defined by three carbon atoms in the ring)
γ(CY) – out of plane bending of the C–Y bond (Y = N, O)
γ(COH) – out of plane bending of the O–H bond (the change in angle between the O–H bond and plane defined by three carbon atoms in the ring)
γ_{im}(CC) – out of plane bending of the C2–C7 (the change in angle between the C2–C7 bond and plane defined by three carbon atoms in the ring)
γ_{im}(CH) – out of plane bending of the C7–H bond
$\delta(NCH_3)$ – combinations of angles N–C8–H, H–C8–H in the N–CH_3 group
τ(CCC) – torsion angle in the ring (change in the dihedral angle between two C–C–C planes in the ring)
τ_{im}(CC) – torsion around the C2–C7 bond
τ(CN) – torsion around the C7=N bond
τ(NC) – torsion around the N–C8 bond

Table 3
The geometry parameters[a] of the HBZA of hydrogen-bonded and open forms calculated by MP2/6-31G(d,p) and B3LYP/6-31G(d,p) methods[b]

	MP2/6-31G(d,p)				B3LYP/6-31G(d,p)			
	HB	PT	HB open	PT open	HB	PT	HB open	PT open
C1–C2	1.416	1.451	1.406	1.480	1.422	1.465	1.409	1.488
C1–C6	1.401	1.436	1.397	1.462	1.404	1.443	1.399	1.463
C2–C3	1.406	1.421	1.402	1.435	1.407	1.426	1.404	1.436
C3–C4	1.388	1.373	1.391	1.365	1.387	1.370	1.390	1.363
C4–C5	1.401	1.420	1.398	1.437	1.403	1.426	1.398	1.438
C5–C6	1.390	1.376	1.394	1.364	1.389	1.371	1.393	1.361
C1–O	1.351	1.283	1.376	1.248	1.340	1.269	1.368	1.241
C2–C7	1.456	1.407	1.470	1.380	1.455	1.403	1.473	1.382
C7=N	1.291	1.317	1.285	1.340	1.285	1.322	1.276	1.341
N–C8	1.453	1.447	1.453	1.450	1.449	1.447	1.449	1.453
C7=N–C8	117.8	124.4	116.1	124.0	119.4	125.2	117.7	124.7
C2–C7=N	122.1	121.2	121.0	127.8	122.5	122.5	122.0	128.2
C1–C2–C7	121.3	118.3	120.3	114.8	120.87	119.0	120.5	115.1
C2–C1–O	122.4	122.2	117.4	123.2	121.8	122.0	117.9	122.7
C1–O–H	106.4	102.8	108.3	–	107.0	103.7	109.0	–
O–H	0.991	1.529	0.965	–	0.999	1.636	0.966	–
H–N	1.743	1.073	–	1.009	1.713	1.053	–	1.011
O···N	2.638	2.492	–	–	2.617	2.551	–	–
OHN	148.2	146.0	–	–	148.4	142.1	–	–

[a] Distances in Å, angles in degrees.
[b] Structural formulas of particular forms are given in Scheme 2.

The average amplitude of ring bonds changes is 0.003 Å for HB open form. When comparing the intramolecularly hydrogen bonded structures, the differences become twice so large (amplitudes of order of 0.006 Å). This shows additional resonance enhancement of intramolecular hydrogen bond in *Schiff* bases of enol form. More pronounced are changes for bonds with atoms participating in formation of the chelate ring. In the open form the C–O distance decreases on 0.003 Å (average value for two methods), while in hydrogen bonded forms – five times more (0.015 Å). The C2–C7 bond transmits the coupling between acid base centres and

decreases by 0.042 Å, but this effect can mainly result from the change of the hybridization of C7 atom. The effect increases, however, in hydrogen bond forms up to 0.053 Å.

The O–H bond length changes very weakly in the open *Schiff* base, but in hydrogen bonded form increases on the average by 0.005 ± 0.003 Å. Both used methods predict also the hydrogen bond O···N distance shortening on 0.072 and 0.107 Å in MP2/6-31G(d,p) and B3LYP/6-31G(d,p) calculations, respectively.

The bonds' alternation occurs to be larger in the open PT form than in the closed one. It shows that formation of intramolecular PT hydrogen bond makes bond lengths distribution more uniform than in the open forms, which is opposite to behaviour of enol forms in *Mannich* and *Schiff* bases.

Detailed examination of Table 3 makes also evident, that for each particular bond length the changes upon the intramolecular hydrogen bond formation are opposite for the molecular and proton transfer states. Formation of the molecular hydrogen bond causes an increase of the amount of *ortho*-quinoid resonance structure, while for the proton transfer state it decreases. The absolute values of increments in PT forms are a few times higher than in molecular ones.

The average effect of bond lengths modification can be characterized by means the variance of ring bond lengths multiplied by 10^6 [21,22].

Table 4
Calculated average bond lengths ($\bar{d}$)[a] and A values[a] of phenol ring in different forms of the HBZA, benzene, phenol and DMAP

Compound		B3LYP/ 6-31(d,p)	MP2/ 6-31(d,p)	B3LYP/ 6-311++(d,p)
Benzene[b]	$\bar{d}$	1.396	1.396	1.394
Phenol[b]	$\bar{d}$	1.397	1.396	1.3943
	A	6.1	3.0	4.1
DMAP[b]	$\bar{d}$	1.399	1.399	1.397
	A	44.0	44.4	35.5
DMAP-open[b]	$\bar{d}$	1.398	1.397	1.396
	A	15.7	7.3	11.8
HBZA				
Enol-open (1)	$\bar{d}$	1.399	1.398	1.397
	A	40.5	24.3	38.8
Enol-closed (2)	$\bar{d}$	1.402	1.400	1.400
	A	137.3	89.6	125.2
PT-closed (3)	$\bar{d}$	1.417	1.413	1.416
	A	1245.0	875.8	1293.2
PT-open (4)	$\bar{d}$	1.425	1.424	1.423
	A	1595.0	1975.0	2274.0

[a] $\bar{d}$ (in Å) concerning parameter A (in Å^2 10^6).
[b] Data for benzene, phenol and DMAP taken from [22].

$$A = \frac{1}{n}\sum_{i}^{n}(d_i - \bar{d})^2 \cdot 10^6.$$

The values of parameter A and the average bond lengths ($\bar{d}$) are shown in Table 4 for the aromatic rings of all forms involved in the study.

Some representative values for *ortho*-dimethylaminomethylphenol (DMAP-*Mannich* base) obtained previously [22] were also included in this table, having in mind a comparison with the values of HBZA. One can mention a considerable increase of parameter A for HBZA upon the formation of intramolecular hydrogen bond, similarly to DMAP. Nevertheless, values of parameter A are a few times larger in *Schiff* bases than in *Mannich* bases for the respective states. Especially strong are effects in proton transfer states – about 10 times larger than for molecular forms (HB). All three levels of calculations lead to the same conclusions corroborating its reliability.

3.3. Modification of the force constants

As it was shown above, closing of the pseudoaromatic chelate ring leads to bond lengths modification. The pattern of these changes implicates the increasing content of *ortho*-quinoid resonance structure in description of the ground state geometry of molecules with intramolecular hydrogen bond. In the most cases the amplitude of changes was not much larger than typical crystallographic standard derivation (0.003–0.004 Å). In order to demonstrate that these results are not artefacts only, one can use an alternative method namely the analysis of the force constants of particular internal coordinates [21]. In researches on *Mannich* bases the correlation between the distance and force constant changes with negative slope was found; the elongation of bond reduces its force constant [21,22]. It was noteworthy to investigate if such correlations existed for *Schiff* bases and if there were any particular features of such dependencies resulting from π-electron coupling.

The MP2 and DFT B3LYP calculations, at basis set 6-31G(d,p), were used for determining of the force constants as in the case of *Mannich* bases [21,22].

Table 5 contains the force constants of particular bonds in internal coordinates calculated by means of PED procedure [39] for all tautomers presented in Scheme 2. For the ring C–C bonds stretching the changes with respect to DMAP [22] show the pattern characteristic for the increase of the content of *ortho*-quinoid forms, similarly as for distance changes (previous section). For the open forms the changes are of order of 1% on the average, while for the bonded forms the increase of *ortho*-quinoid character becomes larger, about 2%. The greater changes are observed for bonds with atoms directly involved in hydrogen bridge formation. For example, the C–O bond force constant

Table 5
The force constants in mdyn/Å^{n-1} rad^{2-n} (where $n = 0$, 1, 2) B3LYP/6-31G(d,p) and MP2/6-31G(d,p) of the HBZA

Internal parameters	MP2/6-31G(d,p)				B3LYP/6-31G(d,p)			
	HB	PT	Enol open	PT open	HB	PT	Enol open	PT open
C1–C2 str.	7.469	6.389	7.220	5.300	7.135	5.703	6.836	4.887
C1–C6 str.	7.199	5.988	7.261	5.304	6.831	5.554	6.923	5.040
C2–C3 str.	7.095	6.623	7.125	6.115	6.783	6.192	6.812	5.823
C3–C4 str.	7.665	8.240	7.522	8.562	7.410	8.097	7.266	8.407
C4–C5 str.	7.246	6.724	7.329	6.132	6.873	6.242	7.016	5.851
C5–C6 str.	7.584	8.074	7.446	8.536	7.343	8.001	7.193	8.411
C1–O str.	7.336	9.297	6.464	11.388	7.407	9.588	6.400	11.329
C2–C7 str.	5.856	8.006	5.485	8.158	5.662	7.569	5.182	7.671
C7=N str.	10.389	9.553	10.655	8.405	10.613	8.919	11.116	8.073
Av. ring bend	1.363	1.377	1.329	1.268	1.376	1.367	1.337	1.301
Av. ring tors.	0.400	0.346	0.327	0.269	0.426	0.346	0.378	0.263
N=C7–C2 bend	1.474	1.805	1.063	0.954	1.521	1.557	1.035	0.930
O–C1–C2 bend	1.447	1.701	1.145	1.202	1.523	1.584	1.153	1.188
C1–C2–C7 bend	1.709	2.290	1.052	1.053	1.771	1.973	1.025	1.026
C6–C1–O out	0.904	0.981	0.611	0.655	1.009	0.984	0.683	0.718
C2–C7–H out	0.606	0.321	0.427	0.222	0.736	0.406	0.515	0.336
C8–N=C7–C2 tors.	0.021	0.006	0.023	0.004	0.019	0.005	0.023	0.004
N=C7–C2–C1 tors.	0.208	0.217	0.226	0.065	0.191	0.178	0.023	0.065
H–O–C1–C2 tors.	0.168	–	0.023	–	0.191	–	0.028	–
X–H[a] str.	6.154	3.388	8.410	7.584	5.444	4.486	8.179	7.269
H–X–C[a] bend	1.272	0.781	0.822	0.856	1.328	0.706	0.806	0.582

For atom labelling see Scheme 1.
[a] Where X = O or N.

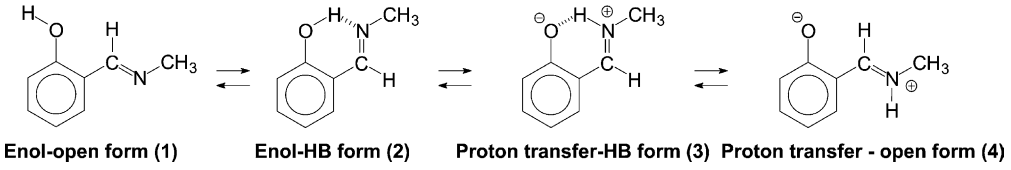

Scheme 2.

increases on 1% in the open form, while in the closed one the increase is 6%. The C2–C7 bond force constant, sensitive to effect of π-electron coupling, increases on the average by 12% in the open form and 16% in the bonded one. Because of the change of the C7=N bond character due to rehybridization of N-atom, the force constant increase exceeds 100%. A pronounced increase of O–C1–C2 (8%), C1–C2–C7 (17%) and C–O–H (7%) bending force constant points out the strengthening of hydrogen bond in *Schiff* bases in relation to *Mannich* bases [21,22].

The O–H bond stretching force constant decreases on average 7%. Interesting, but not clearly understandable is a decrease of many out-of-plane bending and torsion deformations in *Schiff* bases, in relation to *Mannich* bases. It can be brought about more developed steric repulsions of two *N*-methyl groups in *Mannich* bases or from dearomatisation of the ring.

The correlation between force constants modifications and changes of distances resulting from the formation of intramolecular hydrogen bonds appears to be analogous to correlation for *Mannich* bases [21,22]. No specific features are seen for the proton transfer forms, despite the fact that effects are larger and of opposite sign for particular bonds.

The absolute values of increments resulting from the formation of intramolecular hydrogen bond are a few times larger for particular bonds in *Schiff* bases than in *Mannich* bases, which is related to differences in the content of *ortho*-quinoid resonance structures. In this connection the estimation of the content of *ortho*-quinoid structure in particular conformers seems to be an important question.

3.4. Estimation of the content of ortho-quinoid resonance form

Scheme 3 presents the definition of resonance structures for two of the tautomers from Scheme 2. The scheme describes the tautomeric equilibrium between the enol and proton transfer forms. Such a definition appeared [44] very useful in description of the proton

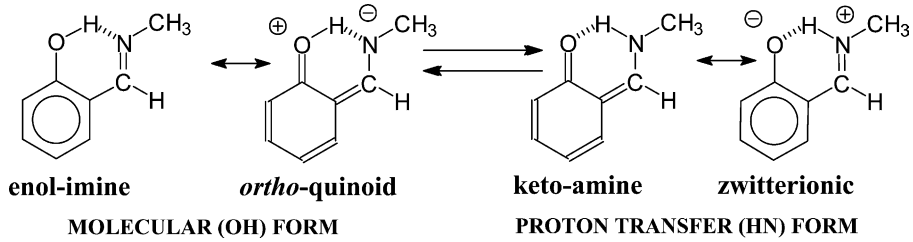

Scheme 3.

transfer equilibrium in *Schiff* bases in solutions, especially in interpretation of UV spectra of proton transfer forms.

As reference states we have not taken theoretical structures with universal standard single and double bond lengths [45,46], but have calculated structures of selected molecules, at the same theory level as the studied tautomers (Scheme 4). *Ortho*-quinone could be proposed as a reference state for the keto structure, but we have selected quinone methide, which is the most often used compound of *ortho*-quinoid character in chemical synthesis and biology [47,48]. Quinone methidine better resembles a structure of *Schiff* bases because it contains the C atom instead of the O atom at position 7. Bond lengths in this structure are given in the molecule **A** in Scheme 4. All parameters were obtained by B3LYP/6-31G(d,p) method that properly describes the spectra and the structure of the studied molecule.

As a second reference state for description of the proton transfer tautomers we have used 2-methyl phenolate (molecule **B** on Scheme 4). Due to different hybridization of the C7 atom, one should avoid using of the C2–C7 bond length in fitting of the resonance structures. We have applied seven bond lengths, six of phenyl ring and the C–O distance. In the description of bonded enol forms the structure **A** is used as a representative of *ortho*-quinoid form and syn *ortho*-toluol as a reference of the "molecular" tautomer (structure **C** on Scheme 4). In the case of the open enol forms (see Scheme 2) the reference state is the anti *ortho*-methyl phenol (structure **D** on Scheme 4).

The calculations of the content of particular resonance structures were performed with the analytical method of simultaneous solution of the set of linear equations, on the condition that each tautomer is a superposition of two resonance structures; X is the content of *ortho*-quinoid structure. Then

$$X = \frac{\sum(y_i - b_i) \times (a_i - b_i)}{\sum(a_i - b_i)^2},$$

where the y_i is a particular distance in a given tautomeric form, a_i – related distance in the structure **A**, and b_i – in selected, non-quinoid second resonance structure.

The results of calculations are as follows: in the open enol form of *Schiff* base a content of *ortho*-quinoid structure is 4.6%, in the closed enol form of *Schiff* base it is 16.7%, in the closed proton transfer form – 40.4% and in the open proton transfer form 70.5%. This comes in full agreement with the previously discussed direct results of the distance and force constants calculations for particular tautomers, so it conforms to non-uniform bonds distribution parameter A given in Table 4. In the open enol form of *Schiff* base only small asymmetry in the ring bond lengths distribution was observed. A very serious participation of resonance in stabilization of the intramolecular hydrogen bond was found in *Schiff* base, which is a real feature of resonance assisted hydrogen bonds [19]. The calculations show that the effect is even larger for the proton transfer hydrogen bonded tautomer. The calculations show approximately equal participation of resonance forms, which is characteristic for the systems with the most effective resonance. This is also responsible for the large red shift of the electronic absorption bands for *Schiff* bases [44]. Within defined here resonance scheme it is hardly to call such a state a keto form [49]. Only for open proton transfer form nearly keto state (70%) can be obtained. The calculations performed at MP2/6-31G(d,p) level give similar estimation of the amount of keto forms. It demonstrates that the conclusions drawn here are not dependent on the level of cal-

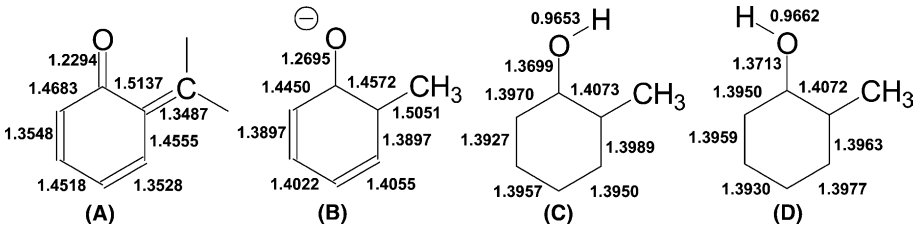

Scheme 4.

culations. The proposed index seems to have more clear meaning as non-aromaticity index of phenyl rings than η parameter [28]. Additionally, the dearomatization of the ring does not necessarily imply pronounced increase of the energy of the whole system because of resonance stabilisation of intramolecular hydrogen bonds.

4. Conclusions

The gas phase IR spectra of the HBZA were measured and calculated by GAUSSIAN 94 program. Comparison of the experimental and calculated frequencies corroborates the reliability of the performed calculations.

In the discussion of the structural consequences of the formation of intramolecular hydrogen bond in *Schiff* bases the effects of the bond differentiation were analysed. Alike in *Mannich* bases, ab initio calculations show that the formation of intramolecular hydrogen bond leads to bond differentiation in the pattern characteristic of *ortho*-quinoid resonance structure. In the case of proton transfer form these effects are much larger. However, opening of the intramolecular hydrogen bond of proton transfer form enhances this differentiation and opposite in molecular (enol) forms. The observed effects have opposite sign of changes for both types of hydrogen bond.

The structural effects were correlated with force constants of particular bonds calculated in internal coordinates. It was shown that correlation is pretty good, shortening of the bond leads to the increase of its force constant.

The method of estimation of the quantity of *ortho*-quinoid form in particular tautomer forms was proposed. This parameter introduces a very strong differentiation between particular species. In the open enol structure the content of this form is evident less than 5% (B3LYP/6-31G(d,p) calculations). Formation of hydrogen bond in *Schiff* bases causes resonance stabilization of intramolecular hydrogen bond, the content of *ortho*-quinoid form increase to about 17%. It turns out that after the proton transfer the intramolecular hydrogen bond in *Schiff* base can be described by 40% of keto form. The affirmation that after the proton transfer one observes keto form appears not completely reliable. The resonance is effective in this type of systems; this phenomenon was also supported by a large red shift of UV bands. This resonance is responsible for some equalization of bonds' lengths distribution, in comparison to the open proton transfer state, where the amount of the *ortho*-quinoid form was estimated as 70%.

Acknowledgements

Authors wish to thank ÖAD for financial support within the Polish-Austrian exchange program and WCSS (Wroclaw) center for providing us with the computational facilities.

References

[1] E. Hadjoudis, Mol. Eng. 5 (1995) 301.
[2] M.Z. Zgierski, J. Chem. Phys. 115 (2001) 8351.
[3] T. Inabe, New J. Chem. 15 (1991) 129.
[4] R. Herzfeld, P. Nagy, Curr. Org. Chem. 5 (2001) 373.
[5] A. Filarowski, A. Koll, T. Glowiak, E. Majewski, T. Dziembowska, Ber. Bunsenges. Phys. Chem. 102 (1998) 393.
[6] A. Filarowski, A. Koll, T. Glowiak, J. Chem. Soc., Perkin Trans. 2 (2002) 835.
[7] Z. Rozwadowski, E. Majewski, T. Dziembowska, P.E. Hansen, J. Chem. Soc., Perkin Trans. 2 (1999) 2809.
[8] K.B. Borisenko, I. Hargittai, J. Mol. Struct. (Theochem.) 388 (1996) 107.
[9] S.M. Aldoshin, L.O. Atovmyan, in: M.A. Poray-Koshic (Ed.), Problemy Kristalokhimii, Nauka, Moscow, 1984, p. 35.
[10] A. Koll, M. Rospenk, E. Jagodzinska, T. Dziembowska, J. Mol. Struct. 552 (2000) 193.
[11] M.Z. Zgierski, A. Grabowska, J. Chem. Phys. 113 (2000) 7845.
[12] A. Grabowska, K. Kownacki, J. Karpiuk, S. Dobrin, L. Kaczmarek, Chem. Phys. Lett. 267 (1997) 132.
[13] M.I. Knyzhansky, A.V. Metelitsa, M.E. Kletskii, A.A. Milov, S.O. Besugliy, J. Mol. Struct. 526 (2000) 65.
[14] E. Hadjoudis, in: H. Bouas-Laurent, H. Dürr (Eds.), Photochromism Molecules and Systems, Elsevier, Amsterdam, 1990.
[15] T. Sekikawa, T. Kobayashi, T. Inabe, J. Phys. Chem. A 101 (1997) 644.
[16] A. Sytnik, J.C. Del Valle, J. Phys. Chem. 99 (1995) 13028.
[17] J. Rhodes, H. Chen, S.R. Hall, J.E. Beesley, D.C. Jenkins, P. Collins, B. Zheng, Nature 377 (1995) 71.
[18] B. Zheng, S. Brett, J.P. Tite, T.A. Brodie, J. Rhodes, Science 256 (1992) 1560.
[19] P. Gilli, V. Ferretti, V. Bertolasi, G. Gilli, in: M. Hargittai, Hargittai (Eds.), Advances in Molecular Structure Research, vol. 2, JAI Press, Greenwich, CT, 1996, p. 667.
[20] A. Filarowski, A. Koll, Vib. Spectr. 17 (1998) 123.
[21] S.M. Melikova, A. Koll, A. Karpfen, P. Wolschann, J. Mol. Struct. 523 (2000) 223.
[22] A. Koll, S.M. Melikova, A. Karpfen, P. Wolschann, J. Mol. Struct. 559 (2001) 127.
[23] H. Lampert, M. Mikenda, A. Karpfen, J. Phys. Chem. 100 (1996) 7418;
J. Phys. Chem. 101 (1997) 2257.
[24] K.B. Borisenko, C.W. Bock, I. Hargittai, J. Phys. Chem. 100 (1996) 7426.
[25] L. Rodriguez-Santiago, M. Sodupe, A. Oliva, J. Bertran, J. Am. Chem. Soc. 121 (1999) 8882.
[26] J. Palomar, J.L.G. De Paz, J. Catalan, Chem. Phys. 246 (1999) 167.
[27] M. Fores, S. Scheiner, Chem. Phys. 246 (1999) 65.
[28] M. Čuma, S. Scheiner, T. Kar, J. Mol. Struct. (Theochem.) 467 (1999) 37.
[29] M. Čuma, S. Scheiner, T. Kar, J. Am. Chem. Soc. 120 (1998) 10499.
[30] C. Cheng, S.F. Shyu, F.S. Hsu, Int. J. Quant. Chem. 74 (1999) 395.
[31] G. Chung, O. Kwon, Y. Kwon, J. Phys. Chem. A 102 (1998) 2381.
[32] H.A. Staab, Einführung In Die Theoretische Organische Chemie, Verlag Chemie, Weinheim, 1962.
[33] B.S. Furnuss, J. Hannaford, P.W.G. Smith, A. Tatchell, Vogel's Textbook of practical Organic Chemistry, Longmans, New York, 1989, pp. 997–999.

[34] M.J. Frisch, G.W. Trucks, H.B. Schlegel, P.M.W. Gill, B.G. Johnson, M.A. Robb, J.R. Cheeseman, T. Keith, G.A. Petersson, J.A. Montgomery, K. Raghavachari, M.A. Al-Laham, V.G. Zakrzewski, J.V. Ortiz, J.B. Foresman, C.Y. Peng, P.Y. Ayala, W. Chen, M.W. Wong, J.L. Andres, E.S. Replogle, R. Gomperts, R.L. Martin, D.J. Fox, J.S. Binkley, D.J. Defrees, J. Baker, J.P. Stewart, M. Head-Gordon, C. Gonzales, J.A. Pople, Gaussian 94, Revision B 3, Gaussian Inc., Pittsburgh, PA, 1995.
[35] (a) C. Moller, M.S. Plesset, Phys. Rev. 46 (1934) 618;
(b) J.A. Pople, J.S. Binkley, R. Seeger, Int. J. Quantum, Symp. 10 (1976) 1;
(c) R. Krishnan, J.A. Pople, Int. J. Quantum, Symp. 14 (1976) 91.
[36] (a) A.D. Becke, J. Chem. Phys. 98 (1993) 5648;
(b) C. Lee, W. Yang, R.G. Parr, Phys. Rev. B 37 (1993) 785.
[37] (a) W.J. Hehre, R. Ditchfield, J.A. Pople, J. Chem. Phys. 56 (1972) 2257;
(b) P.C. Hariharan, J.A. Pople, Theor. Chem. Acta 28 (1973) 213;
(c) M.M. Francl, W.J. Pietro, W.J. Hehre, J.S. Binkley, M.S. Gordon, J.A. Pople, Int. J. Chem. Phys. 77 (1982) 3654.
[38] D. Michalska, D.C. Beńko, A.J. Abkowicz-Beńko, Z. Latajka, J. Phys. Chem. 100 (1996) 17786.
[39] J.M.I. Martin, C. Can Alsenoy, GAR 2 PED, University of Antwerp, 1995.
[40] L.I. Kozhevina, E.B. Prokopenko, V.I. Rybachenko, E.V. Titov, J. Mol. Struct. 295 (1993) 53.
[41] L.I. Kozhevina, E.B. Prokopenko, V.I. Rybachenko, E.V. Titov, Spectrochim. Acta A 51 (1995) 2517.
[42] J.B. Foresman, A.E. Frisch, Exploring Chemistry with Electronic Structure Methods, Gaussian Inc., Pittsburg, PA, 1996.
[43] L.H. Gribov, Intensity Theory for Infrared Spectra of Polyatomie Molecules, Consultant Bureau, New York, 1964.
[44] I. Krol, A. Filarowski, M. Rospenk, A. Koll, J. Phys. Chem., submitted.
[45] (a) A. Julg, P. Francois, Theor. Chim. Acta 7 (1967) 249;
(b) A. Julg, in: E.D. Bregmann, B. Pullman (Eds.), Aromaticity, Pseudoaromaticity and Antiaromaticity, Academic Press, New York, 1971, pp. 383–385.
[46] J. Kruszewski, T.M. Krygowski, Tetrahedron Lett. 36 (1972) 3839.
[47] G.G. Qiao, K. Lenghaus, D.H. Solomon, A. Reisinger, I. Bytheway, C. Wentrup, J. Org. Chem. 63 (1988) 9806.
[48] C. Di Valentin, M. Freccero, M. Sarzi-Amadè, R. Zanaletti, Tetrahedron 56 (2000) 2547.
[49] S. Scheiner, J. Phys. Chem. A 104 (2000) 5898.